Korean J. Chem. Eng., **29**(12), 1802-1805 (2012)
DOI: 10.1007/s11814-012-0097-x

Formation of nanoporous nickel oxides for supercapacitors prepared by electrodeposition with hydrogen evolution reaction and electrochemical dealloying

Myung-Gi Jeong, Kai Zhuo, Serhiy Cherevko, and Chan-Hwa Chung†

School of Chemical Engineering, Sungkyunkwan University, Suwon 440-746, Korea
(*Received 4 May 2012 • accepted 18 June 2012*)

Abstract−Highly nanoporous nickel oxide electrodes were obtained by electrodeposition accompanied by hydrogen evolution reaction and the selective electrochemical dealloying of copper from Ni-(Cu) porous foam. The nanoporous nickel oxide electrodes consequently have numerous dendritic morphologies composed of nanopores with 20-30 nm diameters. The specific capacitances were 428 F g^{-1} for as-deposited Ni-(Cu) foam electrode and 1,305 F g^{-1} for nanoporous nickel-oxide electrode after dealloying process, respectively. This indicates increased surface area by dealloying process leads to innovative increase of specific capacitance.

Key words: Nanoporous NiO Foam Electrode, Dendritic Structure, Hydrogen Evolution Reaction, Electrochemical Dealloying, Supercapacitors

INTRODUCTION

Electrochemical capacitors (ECs) have received attention as excellent energy storage devices which have a high power density, long cycle life, excellent reversibility, wide electrochemical window, large specific capacitance, and fast charge-discharge characteristics [1]. Generally, ECs are divided into electric double layer capacitors (EDLCs) and pseudo-capacitor which show faradaic reactions at the surface of metal oxide (or conductive polymer) as electro-active materials [2]. Among them, the pseudo-capacitor (redox capacitor) exhibits high capacitive and high energy characteristics. There are several metal oxides such as ruthenium oxide [3], nickel oxide [4], manganese oxide [5], cobalt oxide [6], vanadium oxide [7], and their alloyed oxides [8-11] for pseudo-capacitors. Among them, NiO has been widely investigated as alternative material for pseudo-capacitors due to its high pseudo-capacitance behavior and attractive cost compared with ruthenium oxide which has highest electrochemical performance and reversibility [12].

It has been reported that the three-dimensional (3D) structures could improve the electrochemical performance due to the easy transportation properties of protons and electrons between electrodes and electrolytes [13]. In addition, the nanoporous morphology with increased surface area can enhance the pseudo-capacitance because the (charge/discharge) storage mechanism based on pseudo-capacitor materials arises from the reversible redox reactions on the surface of electro-active electrodes. As a facile method can be obtained above all structures, there is the method of electrodeposition accompanying with hydrogen bubbles from hydrogen evolution reaction (HER), which occurs by the reduction of H^+ ions at cathodic overpotential [14,15]. In our previous work, we reported on the facile preparation and the electrocatalytic activities of porous dendritic metal electrodes such as Cu [16], Ag [17,18], Pd [19-21], Pb [22], and Au [23,24] which were prepared by dynamic hydrogen template.

In this work, a dendritic Ni-(Cu) alloy foam was fabricated by electrodeposition in hydrogen evolution reaction. A high cathodic overpotential was applied to the conductive substrate for the generation of vigorous hydrogen bubbles, which could result in numerous dendritic morphologies and increased surface area. Furthermore, the nanoporous dendritic Ni foam was successfully prepared by using selective electrochemical dealloying of copper from Ni-(Cu) alloy. The Ni oxide electrodes obtained by these processes showed an excellent electrochemical capacitance and good stability for supercapacitors.

EXPERIMENTAL

In fact, the nickel itself can be prepared as the porous form structure by electrodeposition with HER at cathodic overpotential [25]. However, we used copper as co-alloyed material to obtain the dendritic morphology as well as the generation of numerous nanopores by simple electrochemical dealloying in sulfuric acid. Typically, the formation of dendritic Ni-(Cu) foam electrode was carried out in a three-electrode cell with Pt/Ti on Si wafer as the working electrode (0.1256 cm^2), Ag/AgCl (3 M NaCl) as the reference electrode, and a platinum electrode (1×4 cm^2) as the counter electrode. The cathodic over-potential of −4 V for 5 min has been applied on Pt/Ti on Si wafer substrate [24] in an electrolyte containing 0.2 M $NiCl_2 \cdot 6H_2O$, 0.01 M $CuSO_4 \cdot 5H_2O$, and 1 M H_2SO_4. Then, to describe the nanoporous nickel electrode, the electrochemical dealloying of copper was carried out on dendritic Ni-(Cu) alloy foam at 0.5 V in 1 M H_2SO_4 solution.

The electrochemical performance was measured with an electrochemical workstation (Zahner® Elektric IM6ex, Germany). The morphology was also analyzed by scanning electron microscope (FESEM), JEOL JSM-7000F (Japan) and transmission electron microscopy (TEM), JEOL JEM-2100F (Japan). X-ray diffractometry (XRD) (Bruker AXS D8 Discover, Germany) with Cu Kα radia-

†To whom correspondence should be addressed.
E-mail: chchung@skku.edu

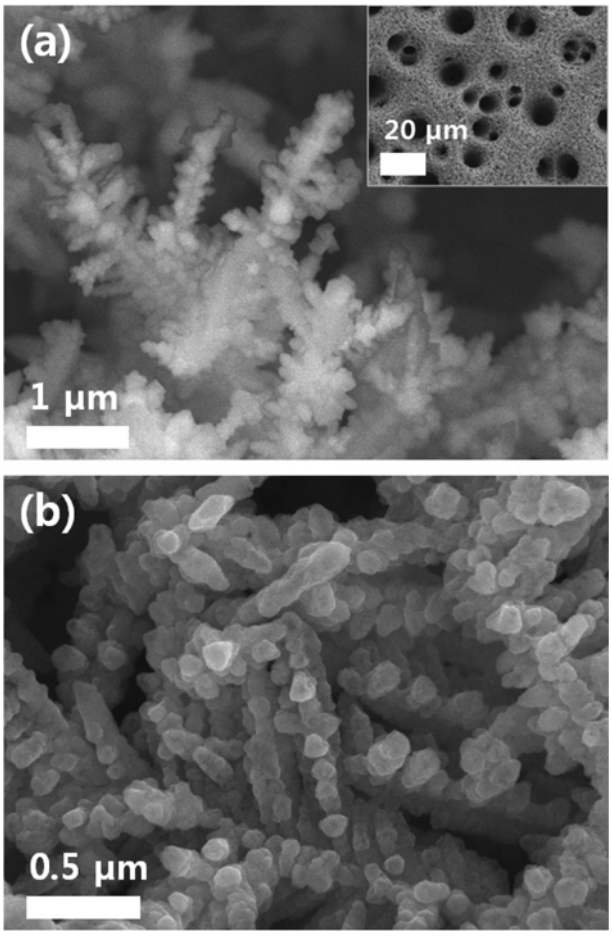

Fig. 1. The FESEM images of (a) the dendritic morphology and top-surface (in inset) of as-electrodeposited Ni-(Cu) foam electrode, (b) the dendritic morphology of Ni-(Cu) oxide foam electrode after annealing at 200 °C for 10 h.

tion at 40 kV and 40 mA was used to evaluate the electrode structures.

RESULTS AND DISCUSSION

Fig. 1(a) shows the FESEM image of Ni-(Cu) foam electrode that was prepared by co-deposition accompanied with hydrogen evolution reaction. As shown in Fig. 1(a), the Ni-(Cu) foam electrode was made up of micropores which have numerous dendiritic morphologies with 100-500 nm size. The elements of nickel and copper as-deposited were 25 at% and 75 at%, respectively. The hydrogen bubbles arising from platinum substrate and/or deposited metal surfaces by cathodic over-potential influence the growth of ramified walls because the metal atoms could not be deposited in the area of hydrogen bubbles. Also, these vigorous hydrogen bubbles lead to the formation of dendritic morphology by the change of hydrodynamic conditions and instability of surface on the near-electrode layer under the non-equilibrium [15,16,26]. According to the above phenomena, the size of dendritic morphology can be controlled by the efficiency of hydrogen evolution, depending on the effect of concentration of metal ions/H^+ ions (H_2SO_4, NH_4Cl, $HClO_4$).

Fig. 1(b) shows FESEM image of the as-prepared Ni-(Cu) foam electrode annealed at 200 °C for 10 h. As a consequence of the above

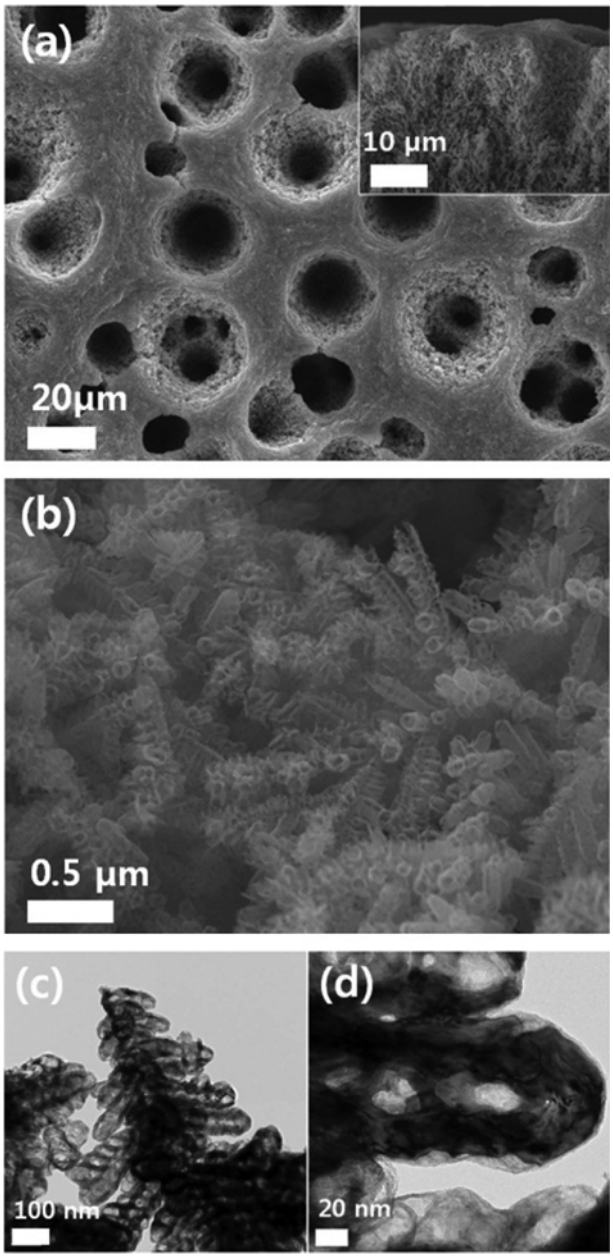

Fig. 2. The FESEM images of (a) the top-surface and the cross-section (inset) of nanoporous nickel foam electrode after electrochemical dealloying, and (b) high magnification of nanoporous morphologies. The pores of 20-50 nm are evident on Ni dendrites in HRTEM images of (c) and (d) after dealloying of copper.

process, the electrode surface area was a little decreased because the copper can be made oxide layer on the metal surface by annealing as shown Fig. 1(b). Fig. 2 shows FESEM images of nanoporous nickel foam which has been processed by electrochemical dealloying at 0.5 V anodic potential in 1 M H_2SO_4. The top-surface of nanoporous nickel foam electrode has less evidence of dendritic morphology (as shown in Fig. 2(a)) compared with Ni-(Cu) foam electrode. This electrode, however, has numerous nanoporous morphology maintaining the initial dendritic structures as shown in Fig. 2(b). Consequently, the surface area of total electrode was increased

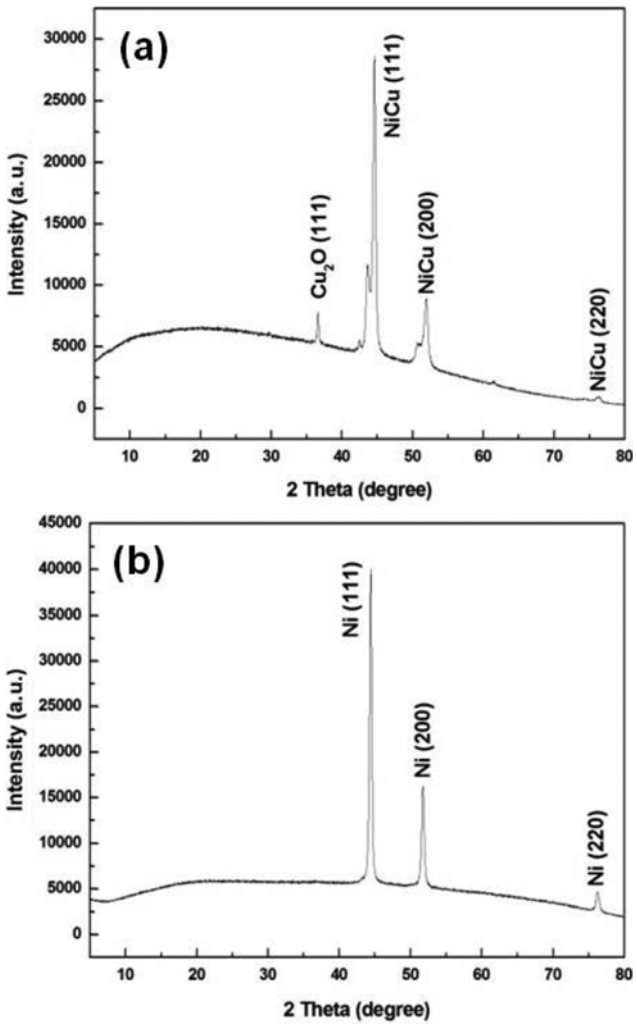

Fig. 3. The XRD peaks of (a) Ni-Cu alloy metal powder, (b) nanoporous Nickel metal powder after electrochemical dealloying in sulfuric acid solution.

by removal of copper from Ni-Cu alloy phase. There are no drastic changes in surface morphology even after annealing process as similar as the Ni-(Cu) oxide foam electrode. The XRD patterns of nanoporous nickel electrode after dealloying are presented in Fig. 3. The peak splitting of the alloy nickel-copper powder electrode occurs in (111), (200), (220) as shown in Fig. 3(a). This indicates that the Ni-(Cu) foam electrode was formed with segregated copper-rich and nickel-rich phases. Fig. 3(b) shows the peak of nanoporous nickel powder from which copper was removed perfectly in sulfuric acid.

The electrochemical performances of the nanoporous NiO foam electrode were characterized by cyclic voltammograms (CV) and galvanostatic charge-discharge in 1 M KOH aqueous solution. The characterization of CV was measured in the three-electrode cell consists of nanoporous NiO foam electrode on the Pt/Ti on Si wafer as the working electrode, a Hg/HgO (1 M NaOH) as the reference electrode and platinum plate (1×4 cm^2) as the counter electrode. Fig. 4(a) shows the typical nickel oxidation/reduction peaks of nanoporous NiO foam electrode in 1 M KOH electrolyte. It is well known that the surface faradaic reaction can occur on NiO electrode according to the following reaction [12]:

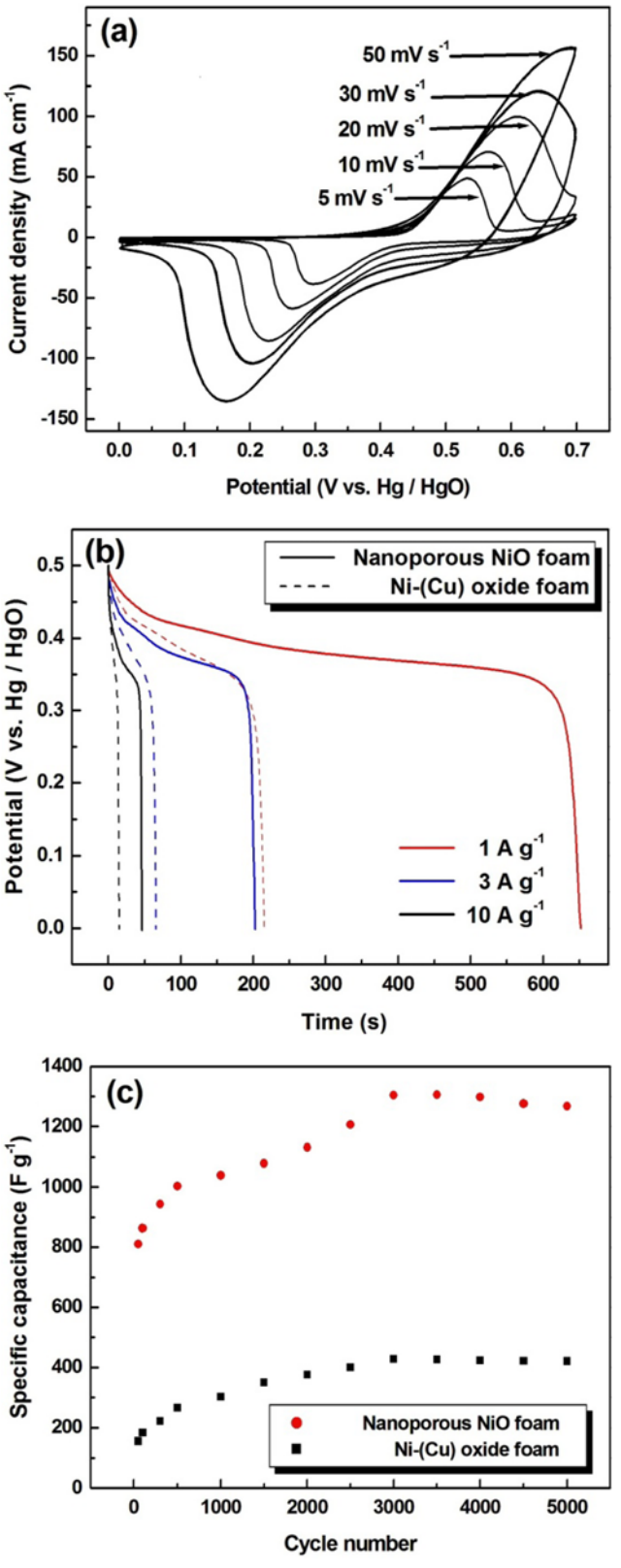

Fig. 4. The electrochemical performance of (a) nanoporous NiO foam electrode after annealing in air at 200 °C at various scan rates 5, 10, 20, 30, and 50 mV s^{-1} between 0.0 and 0.7 V in 1M KOH, (b) the discharge curves on Ni-(Cu) oxide foam electrode and nanoporous NiO foam electrode in potential range of 0-0.5 V, and (c) the stabilities in capacitance during 5000 cycles.

$$NiO+OH^- \leftrightarrow NiOOH+e^-$$

The anodic peak in CV appears due to the oxidation process of NiO to NiOOH, whereas the cathodic peak appears by the reversible reduction process. The charge mechanism of the nanoporous NiO electrode is also related to the oxidation process, while the discharge is of reduction reaction. Fig. 4(b) shows the discharge curves of the Ni-(Cu) oxide foam (the mass of electrode, 0.55 mg) and nanoporous NiO electrode (the mass of electrode, 0.17 mg), which were obtained between 0 and 0.5 V at various current densities of 1, 3, 10 A g^{-1} in 1M KOH electrolyte. A perpendicular variation of the discharge curve below about 0.35 V indicates the double-layer capacitance behavior, and a slope variation of the discharge curve (from 0.5 to 0.35 V) indicates a typical pseudo-capacitance behavior which is caused by redox reaction between electrode and electrolyte. The specific capacitance was calculated from the discharge time using the following equation [4]:

$$Cs=I\Delta t/m\Delta V \quad (1)$$

Where Cs is the specific capacitance, I(A) is the discharge current density applied for Δt (s), and ΔV is the potential in the discharge process. The specific capacitances of the Ni-(Cu) oxide foam electrode at galvanostatic current density of 1, 3, 10 A g^{-1} were calculated as 420 F g^{-1}, 381 F g^{-1}, and 292 F g^{-1}, respectively. On the other hand, the maximum specific capacitance of nanoporous NiO foam electrode was 1,305 F g^{-1} at 1 A g^{-1} and 940 F g^{-1} at 10 A g^{-1}, respectively. This indicates that the increased surface-area by dealloying process leads to innovative increase of specific capacitance. Fig. 4(c) represents the enhanced stabilities of the Ni-(Cu) oxide foam and the nanoporous NiO foam electrodes over 5000 cycles between 0 and 0.5 V at discharging current of 1 A g^{-1}. In both samples, the specific capacitance was increased until 3000 cycle, which is due to their structural properties. The penetration of electrolyte into the inner electro-active electrode through the micro- and nanopores occurs gradually, where the nanoporous dendritic structures is piled up hierarchically.

CONCLUSION

A nanoporous NiO foam electrode was fabricated by electrodeposition with the hydrogen evolution reaction and the simple electrochemical dealloying process. The obtained hierarchical structures of micro-/nano-pores and dendrites present the increase of electrochemical performances for pseudo-capacitor. The maximum specific capacitance of nanoporous NiO foam electrode annealed in air at 200 ºC was measured to 1,305 F g^{-1} at current density 1 A g^{-1}. The good stability in charge/discharge property on this porous electrode also shows the high potential in the application for supercapacitor.

ACKNOWLEDGEMENTS

This research was supported by Samsung Research Fund, Sungkyunkwan University, 2011.

REFERENCES

1. X. Zhao, B. M. Sanchez, P. J. Dobson and P. S. Grant, *Nanoscale*, **3**, 839 (2011).
2. Y. Zhang, H. Feng, X. Wu, L. Wang, A. Zhang, T. Xia, H. Dong, X. Li and L. Zhang, *Int. J. Hydrog. Energy*, **34**, 4889 (2009).
3. T.-S. Hyun, H. L. Tuller, D.-Y. Youn, H.-G. Kim and I.-D. Kim, *J. Mater. Chem.*, **20**, 8971 (2010).
4. Y. Zhang, L. Wang, A. Zhang, Y. Song, X. Li, X. Wu, P. Du and L. Yan, *Korean J. Chem. Eng.*, **28**(2), 608 (2011).
5. C. Yuan, L. Hou, L. Yang, D. Li, L. Shen, F. Zhang and X. Zhang, *J. Mater. Chem.*, **21**, 16035 (2011).
6. X.-H. Xia, J.-P. Tu, X.-L. Wang, C.-D. Gu and X.-B. Zhao, *Chem. Comm.*, **47**, 5786 (2011).
7. V. Augustyn and B. Dunn, *C. R. Chim.*, **13**, 130 (2010).
8. B. Chi, J. Li, X. Yang, Y. Gong and N. Wang, *Int. J. Hydrog. Energy*, **30**, 29 (2005).
9. C. Guan, J. Liu, C. Cheng, H. Li, X. Li, W. Zhou, H. Zhang and H. J. Fan, *Energy Environ. Sci.*, **4**, 4496 (2011).
10. Y. I. Kim, J. K. Yoon, J. S. Kown and J. M. Ko, *Korean Chem. Eng. Res.*, **48**(4), 440 (2010).
11. J. M. Ko and K. M. Kim, *Korean Chem. Eng. Res.*, **47**(1), 11 (2009).
12. P. Justin, S. Kumar Meher and G. Ranga Rao, *J. Phys. Chem. C*, **114**, 5203 (2010).
13. K.-H. Chang and C.-C. Hu, *Appl. Phys. Lett.*, **88**, 193102 (2006).
14. N. D. Nikolic, K. I. Popov, L. J. Pavlovic and M. G. Pavlovic, *J. Eletroanal. Chem.*, **588**, 88 (2006).
15. N. D. Nikolic, G. Brankovic, M. G. Pavlovic and K. I. Popov, *J. Eletroanal. Chem.*, **621**, 13 (2008).
16. S. Cherevko and C.-H. Chung, *Talanta*, **80**, 1371 (2010).
17. S. Cherevko, X. Xing and C.-H. Chung, *Electrochem. Commun.*, **12**, 467 (2010).
18. S. Cherevko and C.-H. Chung, *Electrochim. Acta*, **55**, 22, 6383 (2010).
19. X. Xing, S. Cherevko and C.-H. Chung, *Mater. Chem. Phys.*, **126**, 36 (2011).
20. S. Cherevko, N. Kulyk and C.-H. Chung, *Nanoscale*, **4**, 1, 103 (2012).
21. S. Cherevko, N. Kulyk and C.-H. Chung, *Nanoscale*, **4**, 2, 568 (2012).
22. X. Xing, S. Cherevko and C.-H. Chung, *Appl. Surf. Sci.*, **257**, 8054 (2011).
23. S. Cherevko and C.-H. Chung, *Electrochem. Commun.*, **13**, 16 (2011).
24. S. Cherevko, N. Kulyk and C.-H. Chung, *Langmuir*, **28**, 3306 (2012).
25. X. H. Xia, J. P. Tu, Y. Q. Zhang, Y. J. Mai, X. L. Wang, C. D. Gu and X. B. Zhao, *J. Phys. Chem. C*, **115**(45), 22662 (2011).
26. K. Fukami, S. Nakanishi, H. Yamasaki, T. Tada and K. Sonoda, *J. Phys. Chem. C*, **111**, 1150 (2007).